

### 3.3 $\mu\text{m}$ high brightness LEDs

B. A. Matveev, N. V. Zotova, N.D.II'inskaya, S. A. Karandashev, M. A. Remennyi, N. M. Stus'  
Kovchavtsev A.P., ^Kuryshv G.L.^, Polovinkin V.G.^

Ioffe Physico-Technical Institute RAS, Polytechnicheskaya 26, 194021, St.Petersburg, Russia

^Institute of Semiconductor Physics, Siberian Branch of RAS, Novosibirsk, 630090, Russia

#### ABSTRACT

Deep mesa etching and surface roughening have been implemented to InAs flip-chip LEDs emitting at 3.3  $\mu\text{m}$  (300 K). Near field and power measurements confirmed the output power enhancement of about 2 and brightness increase with an equivalent to a black body temperature of about 1250 K.

#### INTRODUCTION

Recent years have seen extensive research on the mid-IR (2-5  $\mu\text{m}$ ) diodes and one can find publications on resonant cavity [1] and optically pumped [2] as well as on conventional (with point top contact and flat surface) LEDs that have already broken the 1 mW output power barrier that is necessary for most practical applications. Several applications, e.g. spectroscopic measurement with grating, call for sources having high radiance ( $\text{mW}/\text{cm}^2$ ) or apparent temperature values. The epise-down bonded InAs LEDs with broad mirror anode and flat out-coupling surface emitting at 3.3  $\mu\text{m}$  at room temperature have already shown the ability to simulate the black body heated up to 593 K (positive contrast  $\Delta T_a = 300$  K in the 3-5  $\mu\text{m}$  range) [3]. Electrically pumped GaSb/InAs multilayer devices grown onto GaSb also reached the  $\Delta T_a = 300$  K value at 50 mA pump current [4]. Both above examples considered structures with relatively high losses due to total internal reflection at the air/semiconductor interface and it is thus clear that there is still room for device performance improvements.

Deep mesa LED construction narrows the internal radiation diagram due to the reflections from the inclined mesa sidewalls and thus contribute to the out-coupling enhancement. The effect of the above geometrical factor is well known for the InSb negative luminescent devices emitting at 6  $\mu\text{m}$  [5] and efficient NIR and visible LEDs [6], however, to the best of our knowledge there have been no attempts so far to investigate the impact of the mesa dimensions on output power of the mid-IR LEDs with wavelengths in the 3- 5  $\mu\text{m}$  range.

Microtexturing the surface offers enhanced out-coupling efficiency due to suppression of the total internal reflection [2, 6], however, this technology has been not implemented on electrically pumped mid-IR LEDs with wavelengths in the 3 - 6  $\mu\text{m}$  range.

We report on apparent temperature and output power measurements in InAs LEDs with deep mesa and textured out-coupling surface operating at room temperature and grown onto transparent heavily doped  $n^+$ -InAs substrates.

#### EXPERIMENTAL DETAILS

Heterostructures were grown onto heavily doped  $n^+$ -InAs (Sn) (111) ( $n^+ > 10^{18} \text{ cm}^{-3}$ ) substrates transparent to radiation at 3.3  $\mu\text{m}$  due to Moss-Burstein effect and consisted of 2-7  $\mu\text{m}$  thick n-InAs active layers and p-InAsSbP claddings or contact layers. Fig. 1 presents typical composition distribution together with the 77 K band gap scheme; the zero point ( $L=0$ ) corresponds to the  $n^+$ -InAs/n-InAs interface while  $L=6 \mu\text{m}$  indicates the p-InAsSbP/air

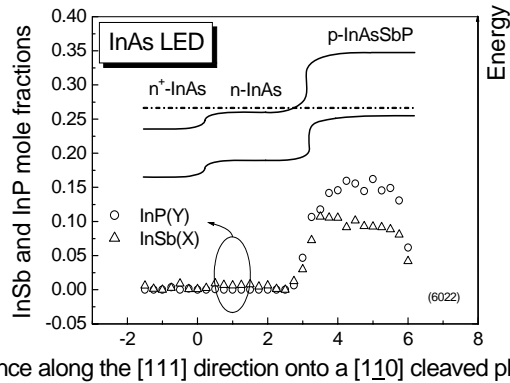


**Fig. 1** Distribution of Sb and P atoms in InAs LED structure (composition profile) together with band diagram.

interface.  $\text{InAs}_{1-x-y}\text{Sb}_x\text{P}_y$  cladding was reasonably lattice matched with InAs substrate ( $y \sim 2.2x$ ) and had an energy gap as big as 460 meV (77 K). Due to the step at the  $n^+$ -InAs/n-InAs interface we could expect hole confinement in n-InAs that is beneficial for the LED operation.

Heterostructure wafers were treated by a multistage wet photolithography process that includes two-stage etching of the mesa and that enables us to prepare flip-chip devices with  $\sim 240 \mu\text{m}$  wide mesa as shown schematically in Fig. 2. A U-like cathode as well as a circular anode ( $D_a = 210 \mu\text{m}$ ) were formed by thermal evaporation of gold films followed by an electrochemical deposition of  $\sim 2 \mu\text{m}$  thick gold layer.

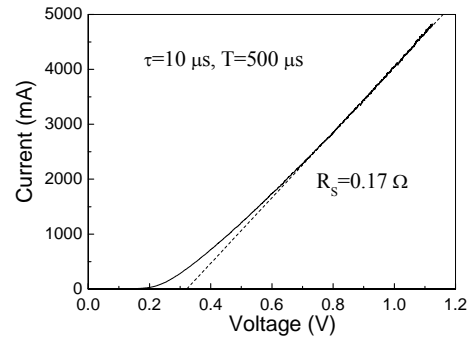
For the sake of a reference some chips lacked one of the etching processes and thus were considered as “shallow” mesa LEDs. The wafers were lapped down to  $\sim 100 \mu\text{m}$  by chemical etching before chip separation.

Fig. 2 (on the right) demonstrates  $0.9 \times 1 \text{ mm}^2$  chip contact surface with  $H_m \sim 40 \mu\text{m}$  deep mesa with  $h_m = 10 \mu\text{m}$  deep cathode contact areas called later as “deep mesa devices”. The chips were further soldered onto silicon submounts with Pb-Sn bonding areas and mounted onto massive copper heatsink.

The devices were biased with pulse currents of  $\tau = 5 - 10 \mu\text{s}$  duration with a repetition rate of  $f = 2 \text{ kHz}$ . A phase sensitive technique together with 77 K cooled CdHgTe or InSb photodiodes were used in electroluminescence (EL) measurements. Common features of the fabricated LEDs were superluminescence and blue shift of the emission spectrum at 77 K due to the dynamic Moss-Burstein effect and superiority of the negative luminescence power conversion efficiency



**Fig. 2** Schematic of the InAs deep mesa “flip-chip” LED grown onto  $n^+$ -InAs and mounted onto Si header (cross section in the N-M direction) (at the left) and photo of the unmounted chip with contacts (at the right).  $D_m$ - is the mesa diameter,  $h_m$ - is the distance from the p-InAsSbP surface to the deepest cathode areas, (“depth of the cathode”),  $H_m$ - is the total depth/height of the internal reflector,  $t$ - is the total p-InAsSbP/n-InAs/ $n^+$ -InAs structure thickness, A- is the anode, C- is the cathode.



**Fig. 3** I-V characteristic of InAs LEDs (300 K)

over the forward one at elevated temperatures (say, at 480 K) due to suppression of the Auger recombination in a depleted active layer similar to the devices described elsewhere [7].

The one dimensional radiation distribution in the vicinity of a LED surface was measured by movable fiber probe, 2-D spatial output distribution was measured by using a thermal imaging microscope on the basis of a hybrid microcircuit of matrix photodetector InAs device that have working range of 2.5 - 3.1  $\mu\text{m}$  [8]. 128 $\times$ 128 photodetector matrix had an inter-element distance of 50  $\mu\text{m}$ . An IR objective with a relative aperture 1:1.8 and 10x optical magnification was used providing the temperature resolution of 0.2 K and 0.015 K for the objects having temperatures 300 K and 450 K, accordingly. The spatial resolution of the device in these conditions amounts to  $\sim 7 \mu\text{m}$  at the diffraction resolution limit of 2.5 – 3.0  $\mu\text{m}$ .

## RESULTS AND DISCUSSION

Fig. 3 presents I-V characteristics showing fairly low serial resistance amounting to 0.17  $\Omega$  due to high conductivity of n<sup>+</sup>-InAs and broad cathode area. Fig. 4 shows IR images of

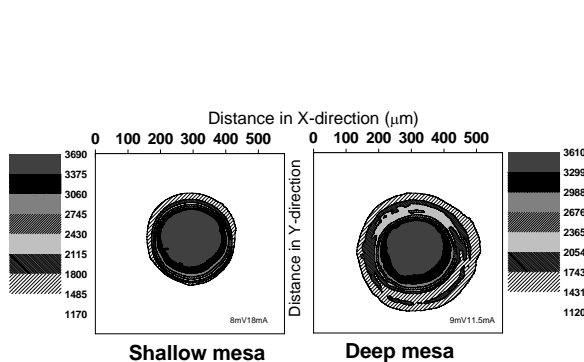


**Fig. 4** IR images of the activated LEDs with shallow (on the left) and deep (on the right) mesas at 18 an 11.5 mA correspondingly. Intensity white-and-black scaling is presented adjacent to the images. Size of each rectangular image is 580 $\times$ 580  $\mu\text{m}^2$ .

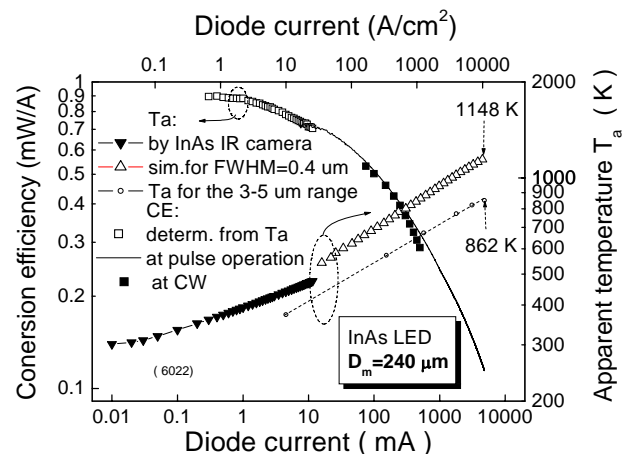


**Fig. 5** Conversion efficiency (CE) (left scale) and apparent temperature (right scale) in a 240  $\mu\text{m}$  wide InAs DH deep mesa LED with flat surface. The latter is presented for the three cases: InAs (77 K) detector (black triangles down, experimental measurements), 3-5  $\mu\text{m}$  band (open circles, simulation) and 3-3.6  $\mu\text{m}$  band (open triangles up, simulations). CE is presented for pulse (solid line) and CW (open and filled boxes) operation modes.

the shallow and deep mesa LEDs measured in the CW mode. It is evident from Fig. 4 that the proposed chip design has positive impact on the output due to reflections from the mesa sidewalls. The latter are seen as additional radiating area around the mesa centre (the radiating ring). From numerical integration using images in Fig. 4 we can conclude that the mesa depth induced enhancement (The Geometrical Enhancement Factor (GEF)) is around 1.3 for the given mesa dimensions.

The evaluation of the apparent temperatures ( $T_a$ ) was performed at CW activation of the LED and was understood as a mean effective temperature of the areas located above the circular anode contact as recorded by a thermal camera. The corresponding  $T_a$  values are presented in Fig. 5 where apparent temperature is plotted as a function of diode current (right scale). In as much as our LEDs emits mainly outside the detector sensitivity band as shown in Fig. 6 the evaluation of the LED power should incorporate the detector “use factor” which amounts to 0.13 meaning that actual LED power is 7.5 times higher than is given by the thermal camera internal calculations/readings. The corresponding calculated values of the output power per unit current (in other words conversion efficiency, mW/A) are plotted in Fig. 7 (left scale). In these estimations we assumed that far field pattern is Lambertian. Conversion efficiency at high pumping currents was estimated using the L-I dependence measured by CdHgTe cooled detector at pulsing conditions (10  $\mu$ s, 2 kHz) (see dotted and solid lines in Fig. 7). Both L-I characteristics for small CW and high pulsed currents were matched in the vicinity of  $I=10$  mA point by adjusting the power data for high current values. As seen from Fig. 5 initially high conversion efficiency in deep mesa LED (0.9 mW/A) degrades down to 0.11 mW/A at high pumping conditions ( $I=5$  A). It is more likely that Joule heating has nothing to do with the above degradation in as much as pulse (solid line) and CW (filled boxes) power coincide up to considerably high current values (500 mA). We are thus attributing the decline of CE to nonradiative losses, namely the Auger recombination. It is frequently assumed that operation at 150 mA is an upper limit for the mid-IR LED [9] and thus the obtained CW operation at 500 mA is a remarkable contribution to the mid-IR LED technology. Indeed, as it follows from Fig. 6 there is no red shift of the emission spectrum on a current pumping increase which is an indication of good heatsink conditions in our LEDs.

The calculations of the apparent temperature included the evaluation of the black body temperature that produced the same as the LED output and had a) a narrow emission spectrum

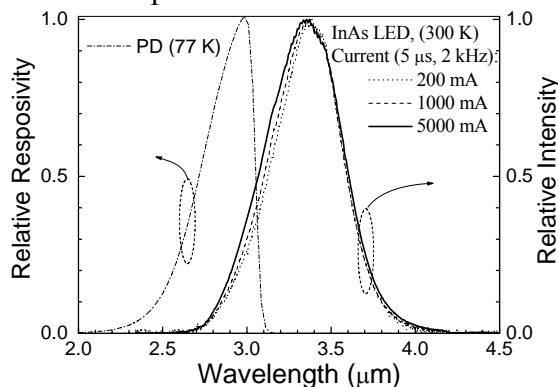


**Fig. 6** Spectral responsivity of cooled InAs detector (dash-dotted line) and room temperature emission spectrum of InAs LED at three pumping conditions:  $I=200$  mA (dotted),  $I=1000$  mA (dashed) and  $5000$  mA (solid line).

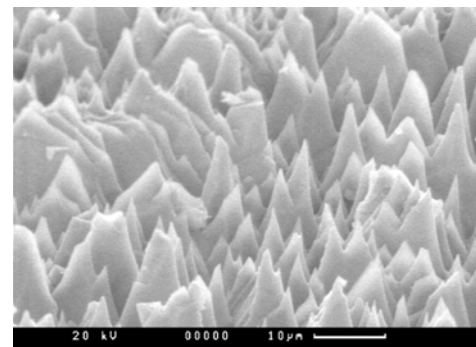


**Fig. 7** Photo of the selectively etched n-InAs(111) out-coupling surface of the deep mesa LEDs. The white horizontal scaling line corresponds to a distance of  $10 \mu\text{m}$ .

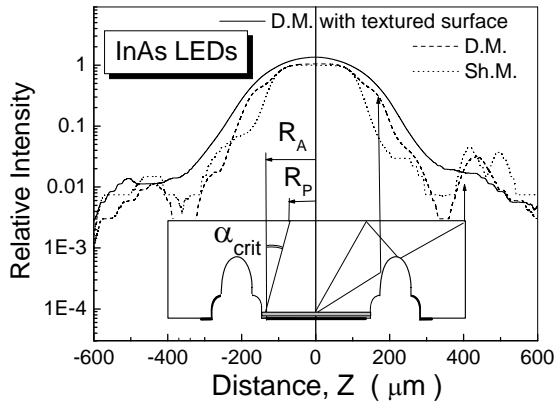


**Fig. 8** Near field radiation distribution in three InAs LEDs at  $I=1$  A: shallow mesa (Sh.M.) LED with flat out-coupling surface (dashed line), deep mesa (D.M.) LED with flat out-coupling surface (dotted line) and deep mesa LED with structured out-coupling surface (solid line) respectively. Arrows show beam paths that form “shoulders” and side peaks.  $R_A$  and  $R_P$  – are the radii of the activated region and “plateau” respectively. The estimated ratio of the effective emitting areas is the following: (1): (1.34): (1.44).

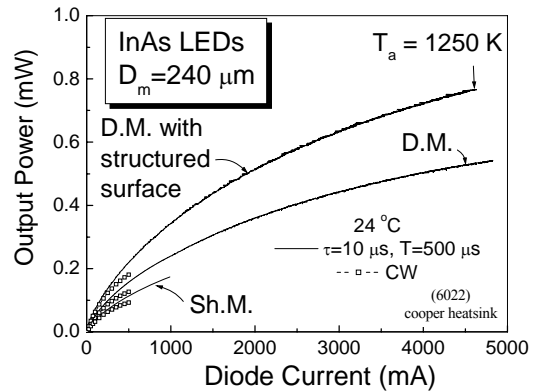


**Fig. 9** Room temperature L-I characteristics of three InAs LEDs with shallow mesa and flat surface, deep mesa with flat surface and deep mesa with structured (selectively etched) surface.

similar to that of the LED under consideration (FWHM=0.4  $\mu\text{m}$ ) or b) emission within the 3-5  $\mu\text{m}$  band. The latter definition is convenient when measuring the  $T_a$  values by HgCdTe or InSb cooled cameras adapted usually to the 3-5  $\mu\text{m}$  atmospheric transparent window, whereas the former definition is used when narrow band detection is of major concern. As seen from Fig. 5 the LED activated at  $I=5$  A is seen as a black body heated up to 1148 K and 862 K for a narrow band and 3-5  $\mu\text{m}$  detectors respectively. The described LEDs are more efficient than reported in [4] (e.g. at  $I=50$  mA: 0.58 mW/A vs 0.11 mW/A respectively) and our maximum apparent temperature values exceed the best published results of 600 K [4] and 593 K [3] for close photonic devices.

Further light extraction increase has been achieved by selective chemical etching of the out-coupling surface resulting in creation cone like structure shown in Fig. 7. The impact of the surface structuring could be found in near field distribution of the output radiation measured in the shallow (dotted line), deep (dashed line) and surface structured deep (solid line) mesa devices shown in Fig. 8. Fig. 8 suggests similar features described previously with respect to IR images shown in Fig. 3 : e.g. emitting dimensions increase due to reflections from mesa side walls marked as an arrow in Fig. 8. As seen from Fig. 8 both shallow and deep mesa devices with flat surfaces have weak side peaks at  $Z=\pm 400$   $\mu\text{m}$  evidently related to the radiation escaping through the sides of the chip and have nearly constant radiance close to the center of the structure just above the anode area ( $Z=0$ ). The “plateau” diameter ( $D_P$ ) relates to active area dimension (in fact to the anode diameter due to the current crowding effect) ( $D_A$ ) and device thickness ( $t$ ) as shown in Fig. 8 and follows simple relation :  $(D_P)=(D_A)-2 \cdot t \cdot \text{tg}(\alpha_{critical})$ ,  $\alpha_{critical}$  – is the critical angle for total internal reflections. The near field distribution for the textured LED has “lost” the plateau which means the substantial decrease of  $D_P$  ( increase of  $(\alpha_{critical})$ ). Indeed the radiating spot at the surface is enlarging as seen as the increase of the FWHM in Fig. 8. In addition to this the structured surface weakly reflects back the normally incident rays as seen as an increase of the radiation intensity at the center of the structure (at  $Z=0$ ).

In Fig. 9 which summarizes the effect of chip geometry on the output power, we present the L-I characteristics for three diodes that differ in mesa depth and out-coupling surface morphology. In accordance with Fig. 9 the output power at certain pumping conditions ( say at  $I=1$  A) is increasing in the following row: (1), (1.38), (1.95) for the shallow mesa LED with flat out-coupling surface, deep mesa LED with flat out-coupling surface and deep mesa LED with structured out-coupling surface respectively. The 4.6 A output power of the latter (best) LED reached 0.76 mW with the corresponding apparent temperature value of 1250 K. The apparent temperature increase ( $\Delta T_a=102$  K) with respect to nonstructured LED (1148 K) appeared to be not very impressive because of the 1.1-fold emitting area increase associated with surface structuring (see Fig. 8).

## SUMMARY

InAs flip chip LEDs emitting at 3.3  $\mu\text{m}$  (300 K) with a deep mesa and a structured outcoupling surface have been fabricated and tested. Two fold power increase has been achieved due to mesa side wall reflection enhancement and total internal reflection suppression with the output power as high as 0.76 mW (4.8 A). Simulated maximum apparent temperature (1250 K) appeared to be higher than any previously published for photonics emitters in the 3-5  $\mu\text{m}$  spectral range.

## ACKNOWLEDGMENTS

The work was supported in part by the SBIR/STTR program with administrative support of the U.S. Civil Research and Development Foundation for the IS of the FSU (CRDF) and by The Foundation for Assistance to Small Innovative Enterprises (FASIE) (projects #5982 and 06-2-H4.2-0201). Two authors (M.R. and N.Z.) are also grateful to the Russian President program for support of young scientists and leading scientific schools (project №MK-1804.2005.2).

## REFERENCES

- 1 A.Green, D.Gevaux, C.Roberts, and C.Philips, *Physica E: Low-dimensional Systems and Nanostructures*, **20**, 531 (2004)
- 2 J. W. Tomm., F. Weik, R. Glatthaar, U. Vetter, J. Nurnus, A. Lambrecht, B. Spellenberg, M. Bassler, M. Behringer, and J. Luft, *Proc.SPIE* **5722** (in print)
- 3 V. Malyutenko, O. Malyutenko, A. Zinovchuk, N.Zotova, S. Karandashev, B.Matveev, M. Remennyi, N. Stus', *Book of abstracts of the MIOMD-VI conference, 2004, St Petersburg, Russia*, (<http://www.ioffe.rssi.ru/MIOMD-VI/miomd-abs.html>)
- 4 N. C. Das, G.Simonis, J.Bradshaw, A. Goldberg, and N.Gupta, *Proc. SPIE* **5408**, 136-143 (2004)
- 5 G.R.Nash, N.T.Gordon, D.J.Hall, M.K.Ashby, J.C.Little, G.Masterton, J.E.Hails, J.Giess, L.Haworth, M.T.Emeny, T.Ashley, *Physica E*, **20**, 540-547(2004)
- 6 V.Zabelin, D.A. Zakheim and S.A. Gurevich, *IEEE J. Quant.Electr.* **40**, 1675-1686 (2004)
- 7 B. Matveev., N. Zotova, N. Il'inskaya, S. Karandashev, M. Remennyi, and N. Stus', *phys. stat. sol. (c)* **2**, 927-930 (2005)
- 8 V.M. Bazovkin, A.A. Guzev, A.P. Kovchavtsev, G.L. Kuryshev, A.S. Larshin, V.G. Polovinkin, "Prikladnaya Phyzika" pp. 97-102 (2005) ( in Russian)
- 9 V.K. Malyutenko. "Maps show hotspots in mid-IR LEDs", <http://optics.org/articles/news/9/4/10> (2003)